Atom–photon momentum entanglement with quantum interference

Rui Guo and Hong Guo*
CREAM Group, School of Electronics Engineering and Computer Science, Peking University, Beijing 100871, China

(Dated: February 2, 2008)

With quantum interference of two-path spontaneous emissions, we propose a novel scheme to coherently control the atom–photon momentum entanglement through atomic internal coherence. A novel phenomenon called "momentum phase entanglement" is reported, and we found, under certain conditions, that more controllable entangled state can be produced with super–high degree of entanglement.

PACS numbers: 03.65.Ud, 42.50.Vk, 32.80.Lg

Introduction.— Entanglement with continuous variable has fundamental importance in quantum nonlocality [1] and in quantum information [2]. Being one of the ways of physical realizations, momentum entanglement plays a unique role in recent studies [3, 4, 5, 6, 7, 8, 9, 10]. In spontaneous emission process, well localized atom–photon entangled wavepacket [3] can be produced due to the momentum conservation, with the degree of entanglement inversely proportional to the linewidth of the transition [3, 4, 5, 6]. Therefore, it is believed, by squeezing the effective transition linewidth, that highly entangled EPR–like state [1] could be produced in free space [5, 6].

Insofar experiments [7], the entanglement information can be extracted by correlated momentum measurements, and it is found that the degree of entanglement is completely detectable with the conditional–unconditional variance ratio [R–ratio in Eq. (7)] for a large variety of physical processes [3, 4, 5, 6, 7, 8]. Therefore, it is straightforward to ask if it is physically possible to produce entanglement beyond this momentum detection, the present work will answer this question. In a typical nearly–degenerated three–level atom, which will be discussed in the following, we find that the interference between different quantum pathways [11, 12] produces significantly the so–called "phase–entangled" state, in which the entanglement information can not be evaluated properly by solely using the momentum detection measure, i.e., the R–ratio. Within this model, we find that not only the degree but also the modes of the entanglement can be effectively manipulated by controlling the atomic internal coherence, and the entanglement degree exhibits, "anomalously", to be proportional to the atomic linewidth of the excited energy levels. Therefore, it is possible to use this proposed scheme to produce a novel and more controllable highly entangled atom–photon system in realistic applications.

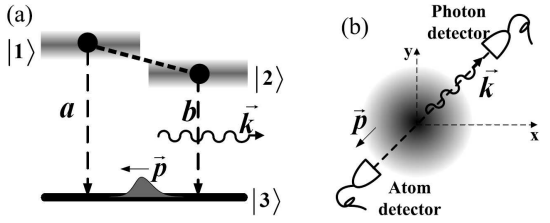

FIG. 1: (a) The atom has two closely–lying upper levels and provides two quantum pathways for the spontaneous emissions. The momentum conservation leads to the entanglement of the emitted photon and the recoiled atom. (b) Schematic diagram for the momentum detection. The two detectors are fixed in one dimension as in the reported experiments [7].

Theoretical model.— As shown in Fig. 1 (a), the three–level atom has two transition pathways "a" and "b" to induce the momentum entanglement with the emitted photon due to momentum conservation. We will, in the following, only consider the strong interference conditions, which assumes that the dipoles $\vec{\mu}_{a,b}$ parallel with each other [11], i.e., $\varepsilon \equiv \vec{\mu}_a \cdot \vec{\mu}_b / |\vec{\mu}_a| \cdot |\vec{\mu}_b| = 1$, and the upper-levels are nearly-degenerated: $\omega_{12} \equiv \omega_a - \omega_b < \gamma_{a,b} \ll \omega_{a,b}$, where $\gamma_{a,b}$ and $\omega_{a,b}$ are the linewidths and central frequencies of the two transitions, respectively. The Hamiltonian of this system with the rotating wave approximation is:

$$\begin{aligned}\hat{H} &= \frac{(\hbar\hat{\vec{q}})^2}{2m} + \sum_{\vec{k}} \hbar\omega_{\vec{k}} \hat{a}^\dagger_{\vec{k}} \hat{a}_{\vec{k}} + \hbar\omega_a \hat{\sigma}_{11} + \hbar\omega_b \hat{\sigma}_{22} \\ &+ \hbar \sum_{\vec{k}} \left[g_a(\vec{k}) \hat{\sigma}_{31} \hat{a}^\dagger_{\vec{k}} e^{-i\vec{k}\cdot\vec{r}} + g_b(\vec{k}) \hat{\sigma}_{32} \hat{a}^\dagger_{\vec{k}} e^{-i\vec{k}\cdot\vec{r}} + \text{H.c.} \right],\end{aligned} \tag{1}$$

where $\hbar\hat{\vec{q}}$ and $\vec{r}$ are the atomic center–of–mass momentum and position operators, m is the atomic mass, $\hat{\sigma}_{ij}$ is the atomic operator, $\hat{a}_{\vec{k}}$ ($\hat{a}^\dagger_{\vec{k}}$) is the annihilation (creation) operator for the kth vacuum mode with wave vector $\vec{k}$ and frequency $\omega_{\vec{k}} \equiv ck$, and $g_{a,b}(\vec{k})$ are the coupling co-

*Author to whom correspondence should be addressed. E-mail: hongguo@pku.edu.cn, phone: +86-10-6275-7035.

efficients for the two transitions, where we use $\vec{k}$ to denote both the momentum and polarization for simplicity.

It is convenient to depict the above interaction system in Schrödinger picture and expand the photon–atom state as:

$$|\psi\rangle = \sum_{\vec{q},n=1,2} \exp\left[-i\left(\frac{\hbar q^2}{2m}+\omega_a\right)t\right] A_n(\vec{q},t)|\vec{q},0,n\rangle + \sum_{\vec{q},\vec{k}} \exp\left[-i\left(\frac{\hbar q^2}{2m}+ck\right)t\right] B(\vec{q},\vec{k},t)|\vec{q},1_{\vec{k}},3\rangle \ , \quad (2)$$

where the arguments in the kets denote, respectively, the wave vector of the atom, the photon, and the atomic internal states.

Using the Born–Markov approximation, the evolution of atom–photon state can be solved from Schrödinger equation. Suppose the atom is initially prepared in a superposed internal state $A_{10}|1\rangle + A_{20}|2\rangle$ with a Gaussian wavepacket $G(\vec{q}) \propto \exp[-(\vec{q}/\delta q)^2]$, and the detections are restricted as in Fig. 1 (b), then the one–dimensional steady state solutions yields:

$$A_1(q,t\to\infty) = A_2(q,t\to\infty) = 0, \quad (3)$$

$$B(q,k,t\to\infty) \propto \exp[-(\Delta q/\eta)^2] \times \left[\frac{C_1(2g_b s_1/\varepsilon\sqrt{\gamma_a\gamma_b}-g_a)}{i(\Delta q+\Delta k)+(s_1/\gamma_a-\frac{1}{2})} + \frac{C_2(2g_b s_2/\varepsilon\sqrt{\gamma_a\gamma_b}-g_a)}{i(\Delta q+\Delta k)+(s_2/\gamma_a-\frac{1}{2})}\right], \quad (4)$$

where the parameters are defined as:

$$s_{1,2} \equiv \frac{1}{2}(\lambda \pm \sqrt{\lambda^2+\varepsilon^2\gamma_a\gamma_b}),\ \lambda = \frac{\gamma_a-\gamma_b+2i\omega_{12}}{2},$$
$$C_{1,2} \equiv \pm\frac{s_{2,1}A_{10}+\frac{1}{2}\varepsilon\sqrt{\gamma_a\gamma_b}A_{20}}{s_2-s_1},\ \eta \equiv \frac{\delta q\hbar k_0}{m\gamma_a}, \quad (5)$$

and the effective wave vectors are defined by:

$$\Delta k \ \equiv\ \frac{k-k_0}{\gamma_a/c}\ ,\ \Delta q \equiv \frac{\hbar k_0}{m\gamma_a}(q-k_0)\ ,\ k_0 = \frac{\omega_a}{c}. \quad (6)$$

Entanglement detection—The nonfactorization of the wavefunction in Eq. (4) reveals the atom–photon entanglement. In both theoretical [4, 9] and experimental studies [7], the ratio of the conditional and unconditional variances [i.e., the R–ratio defined in Eq. (7)] plays a central role, since it is a direct experimental measure of the nonseparability (entanglement) of the system.

With the single–particle measurement, the unconditional variance for the effective atomic momentum is determined as $\delta q^{\rm single} = \langle\Delta q^2\rangle - \langle\Delta q\rangle^2 = \int \mathrm{d}\Delta q\ \mathrm{d}k\Delta q^2|B(q,k)|^2$, where the average $\langle\cdot\rangle$ is taken over the whole ensemble. Meanwhile, the coincidence measurement gives the conditional variance as $\delta q^{\rm coin} = \langle\Delta q^2\rangle_{\Delta k_0} - \langle\Delta q\rangle^2_{\Delta k_0} \propto \int \mathrm{d}\Delta q\ \Delta q^2|B(q,\Delta k_0)|^2$, where the photon is previously detected at some known Δk_0. With these two variances, the entanglement is evaluated by:

$$R \equiv \delta q^{\rm single}/\delta q^{\rm coin} \geq 1. \quad (7)$$

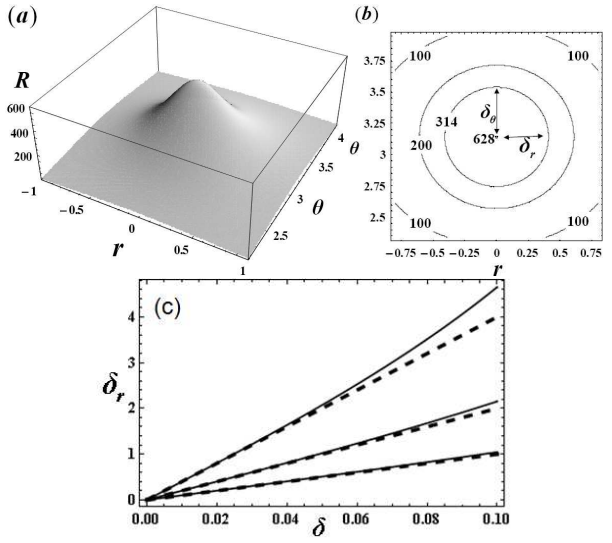

FIG. 2: (a) The "amplitude entanglement" R–ratio is plotted in dependence on the atomic coherence r and θ with $\delta = 0.02$, $\eta = 0.1$. (b) The contour plot of Fig. 2 (a). The circular contours indicate the symmetric roles played by r and θ in controlling the R–ratio. The FWHM is denoted by δ_θ and δ_r as in the figure. (c) The FWHM of $R(r)$ is plotted in solid lines in dependence of δ with $\eta = 0.05, 0.1, 0.2$ from the top to the bottom. Dashed lines are the fitted function $2\delta/\eta$.

Due to the interference of two transition pathways, the R–ratio highly depends on the initial coherence of the two upper atomic levels, which is evaluated by $A_{10}/A_{20} \equiv \exp(r+i\theta)$, where r depicts the relative occupation probabilities of the two upper levels, and θ determines their coherence phase. In further discussions, we assume $\gamma_a = \gamma_b \equiv \gamma$, and define $\delta \equiv \omega_{12}/\gamma < 1$ for simplicity.

Following the above analysis, the dependence of R on r and θ is illustrated in Fig. 2. Under the conditions $\eta \ll 1$ and $\delta^2/\eta \ll 1$ [13], we find that $R(r,\theta)$ can well be approximated by Lorentzian function, and the parameters r and θ, in spite of their quite different physical essences, play very symmetric roles in controlling the detectable R–ratio [Fig. 2 (b)]. Under these conditions, the R–ratio is maximized at the dark state coherence $[(|1\rangle - |2\rangle)/\sqrt{2}]$:

$$R_{\max} = R(r=0,\theta=\pi) \approx \sqrt{2\pi}\eta/\delta^2, \quad (8)$$

the full width at half maximum (FWHM) of which can be well approximated by $\delta_r \approx \delta_\theta \approx 2\delta/\eta$, as shown in Figs. 2 (b) and (c). Therefore, with properly chosen atomic parameters η and δ, this scheme could be used to produce significant detectable entanglement in a relatively large range of the initial atomic coherence. For example, with $\eta = \delta = 0.01$, the system with $R > 100$ can be produced within the range of $0.018 < |A_{10}/A_{20}|^2 = e^{2r} < 55$, and $0.36\pi < \theta < 1.6\pi$.

Phase entanglement.— For a bipartite pure–state system, the degree of entanglement can be completely eval-

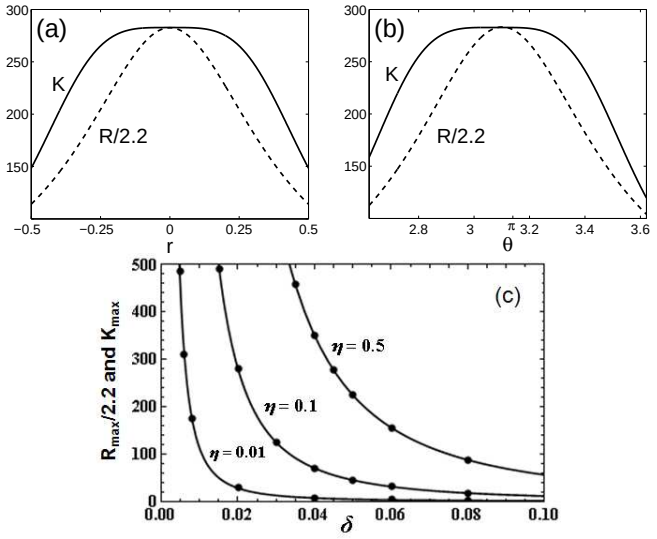

FIG. 3: Plots of K and $R/2.2$ in dependence on the atomic coherence r or θ, where $\eta = 0.1$, $\delta = 0.02$. (a) θ is fixed at π. (b) r is fixed at 0. (c) K (in spots) and the function $R/2.2$ (in solid line) are plotted at the dark–state coherence $r = 0$ and $\theta = \pi$.

uated by the Schmidt number [3, 14]

$$K \equiv 1/\sum_n \lambda_n^2 \geq 1, \tag{9}$$

where λ_n's are eigenvalues for the entangled atomic modes $\psi_n(q)$ and photonic modes $\phi_n(k)$ in the Schmidt decomposition [15]: $B(q,k) = \sum_n \sqrt{\lambda_n}\psi_n(q)\phi_n(k)$.

In previous studies on atom–photon momentum entanglement [3, 4, 5, 6], the R–ratio well measures the entanglement since one has $R \propto K$. However, this is not true when the quantum interference is strong as shown in this model: since the R–ratio is constructed from the module part of the wavefunction, it reveals only the amplitude correlation between two particles' momentum; therefore, when the phase is critical for the nature of the entanglement due to the interference, the traditional R–ratio measurement becomes inadequate for detecting the full entanglement information. Actually, by controlling the interference with the atomic internal coherence, one may produce two systems with $K > K'$ whereas $R < R'$, which indicates that significant entanglement information may be lost by the momentum detection with only the R–ratio.

We compare K and R in Fig. 3, from which one finds that both of them are maximized at the dark-state coherence ($r = 0$, $\theta = \pi$). However, compared with $R(r,\theta)$, $K(r,\theta)$ exhibits a much slower decay in the vicinity of the maximum, which indicates that, with different initial atomic coherences, some entanglement information may be transferred into the "phase" and can not be measured only by the amplitude–based detections. This phenomenon is particularly important for some highly entangled states, e.g., under the condition $\delta = 2 \times 10^{-3}$, $\eta = 0.1$, $r = 0$, $\theta = \pi$, one may prepare a highly entangled state with $K \approx 2.8 \times 10^4$ and $R \approx 6.2 \times 10^4$; however, when the initial atomic momentum and coherence change to $\eta' = 2\eta, r' = 0.13$, the entanglement of the system does not change, i.e., $K' = K$, but the R-ratio detection shows that $R' = 0.05R$. This shows that some entanglement information of the system is transferred into the phase.

Similar phenomenon of the so–called "phase entanglement" has been reported recently in the position space [4, 9, 10]: due to the spreading of the wavepacket, it appears instantly and must be detected by a series of spatial measurements in time [9]. For the momentum "phase entanglement" in this scheme, however, since it is caused by the quantum interference and is not affected by the wavepacket's spreading, this phenomenon keeps steady in time and could be much easier to be directly observed in experiments [7].

It is possible to evaluate the "phase entanglement" for the highly entangled states in this scheme. For the entanglement maximized at the dark–state coherence, the wavefunction takes a similar form as if no interference occurs [3, 4, 5, 6]:

$$B(q,k,t\to\infty) \propto \frac{\exp\left[-(\Delta q/\eta)^2\right]}{i(\Delta q + \Delta k) - \delta^2/4}\ , \tag{10}$$

and then the Schmidt number yields:

$$K_{\max} \approx 1 + 0.28(4\eta/\delta^2 - 1). \tag{11}$$

Together with Eq. (8), one yields the relation

$$K_{\max} = K(r=0,\theta=\pi) \approx \frac{R_{\max}}{2.2} \approx \frac{1.12\hbar k_0 \delta q \gamma}{m\omega_{12}^2}, \tag{12}$$

well fulfilled for $\eta/\delta^2 \gg 1$ and $\eta \ll 1$ [13], as shown in Fig. 3 (c). The linear relation between $K_{\max}$ and $R_{\max}$ shown in Eq. (12) indicates that the entanglement is completely detectable with fixed dark–state coherence $r = 0$ and $\theta = \pi$. For general conditions (where r and θ take arbitrary values, see Fig. 3), we have $K \geq R/2.2$. Therefore, the degree of "phase entanglement" can be evaluated by the following parameter:

$$PE \equiv 2.2K/R \geq 1, \tag{13}$$

which is valid for the states produced with different control parameters η, δ, r and θ.

A traditional idea to enhance the entanglement of momentum is to correlate the atom and photon momentum by squeezing the transition linewidth since $K \propto 1/\gamma$ [3, 4, 5, 6]. However, in our proposed scheme, which employs an essentially different mechanism for producing the entanglement through quantum interference, we have, anomalously, that $K_{\max} \propto \gamma$ as shown in Eq. (12). With broader linewidth of the two upper energy levels, the interference will be enhanced and, as a result, increases the momentum entanglement. Therefore,

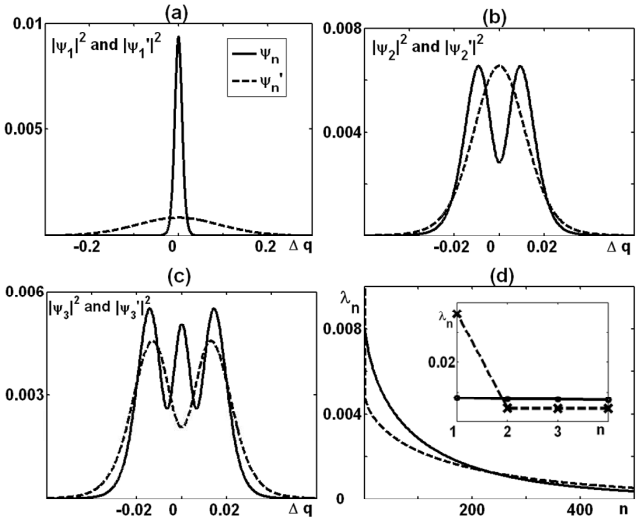

FIG. 4: (a) to (c) First three Schmidt modes are compared between states $B(q,k)$ with $\delta = 0.02$, $\eta = 0.12$, $r = 0$, $\theta = \pi$ and $B'(q,k)$ with $\delta' = \delta$, $\theta' = \theta$, $\eta' = 0.2$, $r' = 0.38$, where one has $K' = K$ and $R' \approx 0.38R$. The phase entanglement of $B'(q,k)$ broadens its first Schmidt mode and decreases the number of peaks for the rest modes. (d) The distributions of the eigenvalues in their Schmidt decompositions, where the inset shows the first four eigenvalues. The solid and dashed lines are for $B(q,k)$ and $B'(q,k)$, respectively.

it is possible to use this mechanism to produce super–high momentum entanglement even for the atomic system with large damping rate γ.

Entangled modes.—The phase entanglement can, more intuitively, be understood in terms of Schmidt decomposition. According to Eq. (9), K is a measure for the number of the important Schmidt modes, while R–ratio is related to the coherence between these modes $[\psi_n(q)]$', which can be seen more clearly by rewriting the unconditional and conditional variances as: $\delta q^{\rm single} = \int {\rm d}\Delta q\ \Delta q^2 \sum_n \lambda_n |\psi_n(q)|^2 = \langle \Delta q^2 \rangle_{E_{\rm i}}$, $\delta q^{\rm coin} \approx \int {\rm d}\Delta q\ \Delta q^2 |\sum_n \sqrt{\lambda_n}\psi_n(q)|^2 = \langle \Delta q^2 \rangle_{E_{\rm c}}$. These formulae indicate that the unconditional variance $\delta q^{\rm single}$ is the variance taken by an "incoherent" superposition of different Schmidt modes weighed by λ_n, i.e., $E_{\rm i}(q) \equiv \sum_n \lambda_n |\psi_n(q)|^2$, while the conditional variance $\delta q^{\rm coin}$ is taken over a "coherent superposition" of different modes, i.e., $E_{\rm c}(q) \equiv |\sum_n \sqrt{\lambda_n}\psi_n(q)|^2$. Therefore, the R–ratio defined in Eq. (7) actually represents the wavepacket narrowing caused by the coherence between different Schmidt modes.

In Fig. 4, we compare the atomic Schmidt modes between the states $B(q,k)$ and $B'(q,k)$ with $K' = K$ and $R' \approx 0.38R$. It can be seen that the phase entanglement significantly broadens the first few Schmidt modes and decreases the number of peaks for the rest ones; moreover, the coherence between different Schmidt modes diminishes and, as a result, decreases the R–ratio. The photonic Schmidt modes exhibit similar properties as atomic modes and remain the Gaussian localization properties [3, 5] in spite of the shape distortions caused by the interference. Therefore, it is possible to apply this scheme to efficiently control the entangled modes under a certain degree of entanglement.

Conclusion.— In summary, we investigate the atom–photon momentum entanglement caused by the quantum interference in a three–level atom. The novel phenomenon of "momentum phase entanglement" is shown and evaluated quantitatively. Using this scheme, a novel atom-photon entangled state can be produced with super–high degree of entanglement and controllable entangled modes. Since the proposed configuration has been extensively studied both theoretically and experimentally [11, 12], and can be realized by mixing different parity levels or by using dressed-state ideas, these new features are most probable to be examined in experiments and used in realistic applications [2].

This work is supported by the National Natural Science Foundation of China (Grant No. 10474004), National Key Basic Research Program (Grant No. 2006CB921401) and DAAD exchange program: D/05/06972 Projektbezogener Personenaustausch mit China (Germany/China Joint Research Program).

[1] A. Einstein, B. Podolsky, N. Rosen, Phys. Rev. **47**, 777 (1935); J. C. Howell *et. al.*, Phys. Rev. Lett. **92**, 210403 (2004).
[2] S. L. Braunstein and P. V. Loock, Rev. Mod. Phys. **77**, 513 (2005).
[3] K. W. Chan, C. K. Law, and J. H. Eberly, Phys. Rev. Lett. **88**, 100402 (2002).
[4] M. V. Fedorov *et. al.*, Phys. Rev. A **72**, 032110 (2005).
[5] K. W. Chan *et. al.*, Phys. Rev. A **68**, 022110 (2003); J. H. Eberly, K. W. Chan and C. K. Law, Phil. Trans. R. Soc. Lond. A **361**, 1519 (2003).
[6] R. Guo and H. Guo, Phys. Rev. A **73**, 012103 (2006).
[7] M. D. Reid and P. D. Drummond, Phys. Rev. Lett. **60**, 2731 (1988); Michael S. Chapman *et al.*, Phys. Rev. Lett. **75**, 3783 (1995); Christian Kurtsiefer *et al.*, Phys. Rev. A **55**, R2539 (1997).
[8] R. Guo and H. Guo, Phys. Rev. A **76**, 012112 (2007).
[9] M. V. Fedorov *et al.*, Phys. Rev. A **69**, 052117 (2004).
[10] arXiv: K. W. Chan and J. H. Eberly, quant–ph/0404093.
[11] S. Y. Zhu and M. O. Scully, Phys. Rev. Lett **76**, 388 (1996); H. R. Xia, C. Y. Ye, and S. Y. Zhu, Phys. Rev. Lett. **77**, 1032 (1996).
[12] M. O. Scully, S. Y. Zhu and A. Gavrielides, Phys. Rev. Lett. **62**, 2813 (1989); S. Y. Zhu, R. C. F. Chan and C. P. Lee, Phys. Rev. A **52**, 710 (1995).
[13] In typical atomic system, η is of the order 0.1 or smaller, e.g., for sodium, one has $\eta \approx 0.05$; moreover, the condition $\delta^2/\eta \ll 1$ is equivalent to $K_{\rm max} \gg 1$, which is our

major concern.

[14] C. K. Law, I. A. Walmsley, and J. H. Eberly, Phys. Rev. Lett. **84**, 5304 (2000); C. K. Law and J. H. Eberly, Phys. Rev. Lett. **92**, 127903 (2004).

[15] R. Grobe *et al.*, J. Phys. B **27**, L503 (1994); S. Parker *et al.*, Phys. Rev. A **61**, 032305 (2000).